Adv. Polar Upper Atmos. Res., **18**, 65–76, 2004

Observation of ionospheric Alfvén resonance at a middle latitude station

Masashi Hayakawa[1], Oleg A. Molchanov[2], Alexander Yu. Schekotov[2] and Evgeny Fedorov[2]

[1] *University of Electro-Communications, Chofu-shi, Tokyo 182-8585*
[2] *Institute of Physics of the Earth, Russian Academy of Science, Moscow, Russia*

(Received November 17, 2003; Accepted March 30, 2004)

Abstract: This paper intends to report on the statistical results on the spectral resonance structures of the ionospheric Alfvén resonances (IAR) in the ULF frequency range 0.1–5.0 Hz on the basis of the analysis of long-term data obtained from July 2000 to December 2002 (2.5 years) at the Karimshino station (Kamchatka, Russia) (L=2.1) by the conventional 3-component search-coil magnetometer. We analyze both the dynamic spectra of three components and polarization spectra in order to distinguish IAR from other possible noises. The average frequency difference ΔF between the adjacent maxima, intensity and occurrence rate of the IAR spectra have been estimated from the averaged spectra.

Early papers at middle latitudes have been based on a small data base. Based on our first long-term observation at middle latitude, new findings, especially related to the seasonal variation, have emerged from this analysis. (1) There is an evident seasonal variation in the occurrence rate with a maximum in the September–January period and an almost complete absence of IAR structures in the spring-early summer time. (2) Occurrence maximum in the diurnal variation is found at 21–23 LT in the autumn and winter. Almost all the IAR structures are observed at local nighttime. (3) The averaged ΔF is found to be about 0.2–0.5 Hz in the autumn period but it seems to increase up to 0.5–0.7 Hz in winter. (4) The IAR occurrence rate is inversely correlated with the *Kp* index of global magnetic activity. (5) The intensity of *D* component exceeds essentially that of *H* component of the IAR structures in a majority of cases. Diurnal variations of resonance frequencies in the *H* and *D* components are not always identical.

Finally the mechanisms to explain the observed characteristics of the IAR have been discussed.

key words: ionospheric Alfvén resonator (IAR), ionosphere, magnetosphere, polarization

1. Introduction

There are different kinds of resonance phenomena in the near-Earth environment. From the higher frequency there is a tranverse resonance in the Earth-ionosphere waveguide in the ELF and VLF range (known as tweek cutoff) (*e.g.* Alpert, 1974; Nickolaenko and Hayakawa, 2002). When we go to the lower frequency down to ELF range, we know the

presence of longitudinal resonance in the Earth-ionosphere waveguide, which is known as Schumann resonances (Nickolaenko and Hayakawa, 2002). Its fundamental frequencies are 8, 14, 20 Hz etc. and recently the observation of the Schumann resonance intensity is found to serve as a kind of global thermometer (*e.g.* Nickolaenko and Hayakawa, 2002).

At the frequency below the Schumann resonance region, there is an additional resonance phenomena called "Ionospheric Alfvén Resonator" (abbreviated as IAR). Polyakov (1976) and Polyakov and Rapoport (1981) predicted theoretically the existence of such Alfvén quasi-resonances in the ionosphere based on the similar considerations.

The IAR plays an important role in the understandig of the physical phenomena in the coupled magnetosphere-ionosphere system (*e.g.* Trakhtengertz and Feldstein, 1991; Lysak, 1991; Pokhotelov *et al*., 2000, 2001; Trakhtengretz *et al*., 2000a,b; Demekhov *et al*., 2000a,b).

The IAR was discovered at a middle latitude station (Nizhni Novgorod, Russia) and at a high latitude station (Kilpisjarvi, Finland) by Belyaev *et al*. (1987, 1990, 1999). Recently experimental evidence for the existence of IAR at high latitudes was confirmed by Demekhov *et al*. (2000a) by using the data at Kilpisjarvi observatory ($L=6$). Yahnin *et al*. (2003) have studied diurnal and seasonal variations of SRS (spectral resonance structure) occurrence rate based on continuous observations for more than 4 years at a high lalitude station, Sodankylä ($L=5.2$). They have found a clear tendency of decrease in both the resonant frequencies and difference ΔF from the minimum to maximum solar activity. The high-resolution measurements of IAR signatures during half a year were made also at a low-latitude station in Crete ($L=1.3$) by Bösinger *et al*. (2002).

In the present paper the statistical properties of the SRS of IAR are analyzed on the basis of the results of continuous observations for more than 2 years at a mid-latitude observatory at Karimshino (Kamchatka, Russia, $L=2.1$), to be compared with the corresponding results at high ($L=5.2$) and low ($L=1.3$) latitudes. Because the latitudinal effect seems to be the most important factor to elucidate the generation mechanism of IAR.

2. Observations and data processing

The continuous registration of the ULF magnetic field variations at the geophysical observatory, Karimshino started in June 2000. The observatory is located in Karimshino (52.94°N, 158.25°E, $L=2.1$) at a distance of about 50 km from Petropavlovsk-Kamchatsky (see the details in Uyeda *et al*., 2002). Three axial induction magnetometer is used to measure geomagnetic field variations in the frequency range 0.003–40 Hz. The sensitivity threshold is better than 20 pT/Hz$^{1/2}$ at a frequency of 0.01 Hz, and it corresponds to 0.02 pT/Hz$^{1/2}$ at the frequencies above 10 Hz. Sampling rate per channel is 150 sp/s, and sampling resolution is 24 bit. The accuracy of absolute and relative (between channels) timing of digital data is 5 ms and better than 10 μs respectively. This station is intended for the study of seismo-electromagnetic phenomena (Gladychev *et al*., 2002), but our ULF observation has yielded interesting results on IAR as well.

Because of relatively high crust conductivity in the region of observations the vertical magnetic signal amplitude is low in comparison with the horizontal one. The amplitude of the vertical component in the frequency range 1–3 Hz is comparable with the sensor sensitivity. Thus, the resonant structures cannot be detected for the vertical component with the

equipment used. The technique and results of the signal analysis for two horizontal components are presented below.

The signal spectra were calculated with the Welch's method in the range 0.1–5 Hz with the frequency resolution 0.05 Hz in the time window 30 min and many parameters of resonance structures were estimated. An example of the evolution of nighttime dynamic frequecy spectra is shown in Fig. 1 for about one week from 12 to 18, September 2000. The bottom three panels illustrate the dynamic spectra for the three magnetic field components (*H*, *D* and *Z*) respectively. The second (from the top) panel indicates the coherency between the two magnetic components *H* and *D* and the third panel indicates the wave polarization by using the two horizontal magnetic field components. The top panel indicates the temporal evolution of *Kp* index (geomagnetic activity) and *Ks* index (indicating the effect seismic effect) (this index is not used in this paper) for comparison. Fig. 2 is another type of presentation of Fig. 1 in the form of spectral power density versus wave frequency for the two horizantal components (*D* (in thick line) and *H* (in thin line). The local time is changed from LT = 19 h to LT = 06 h on a particular day of 13/14 September 2000. We can recognize from this figure the IAR spectra with typical resonance structures especially in the local time interval from LT = 21 to 01, but weak (not so conspicuous) resonance structures

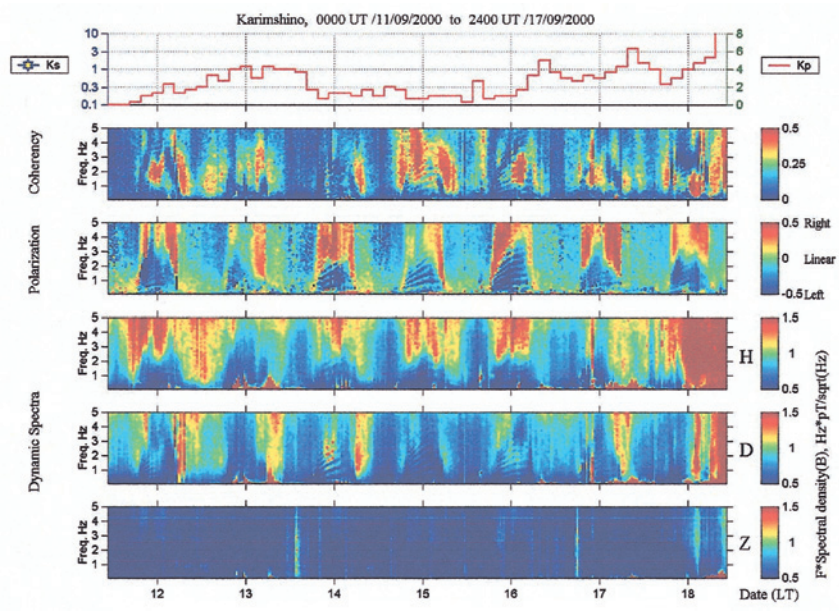

Fig. 1. An example of the temporal evolution of SRS of IAR from LT=19 to 06 h on 13–14 September, 2000. SRS is most clearly seen at LT=22 h (ΔF~0.5 Hz). LT=UT+12 h. The top panel indicates the Ks and Kp index, the second one, coherency between the horizontal magnetic field components, the third, wave polarization by means of the horizontal magnetic field components, and the last three panels, the dynamic spectra for H, D and Z components. The values are indicated in color.

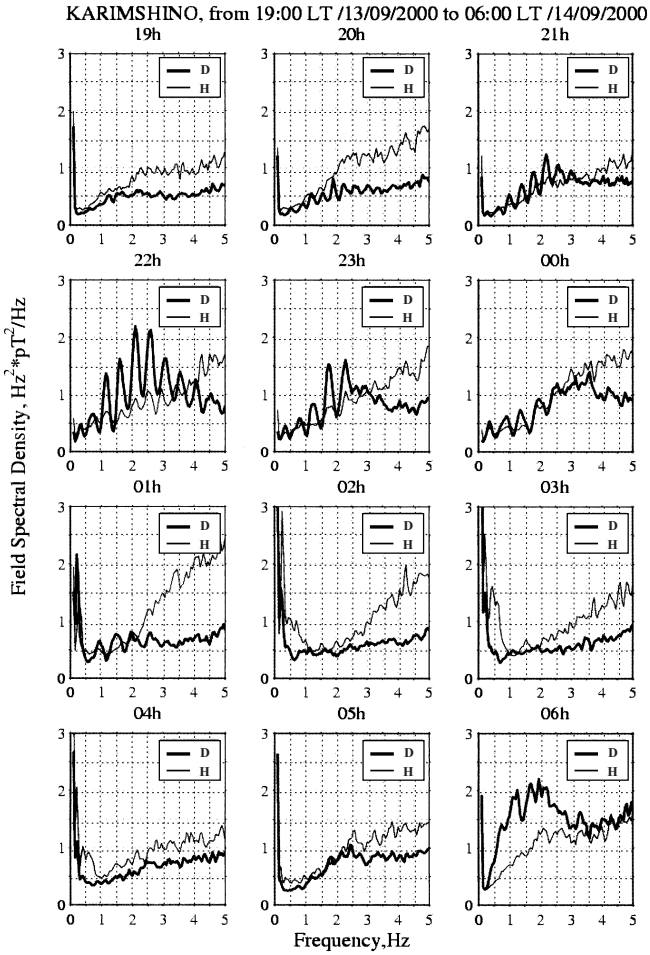

Fig. 2. An example of temporal evolution of dynamic spectra of ionospheric Alfvén resonances on a particular day (13/14 September 2000).

are also seen at other LT's.

We can notice from Figs. 1 and 2 that we can find very clear resonance structures on the horizontal magnetic field components (*H* and *D*). However, when we use the polarization spectrum, it is much easier for us to identify such resonance structures, which is clearly recognized in the 2nd top panel of Fig. 1, when we compare it with the corresponding amplitude dynamic spectra (*e.g.* the 2nd panel from the bottom in Fig. 1). The wave is found to be left-handed polarized.

The algorithm of automatic SRS detection and calculation of its main parameters have been developed in this paper and have been described below. Various parameters obtained from the analysis of the spectra are as follows:

- averaged frequency difference ΔF,

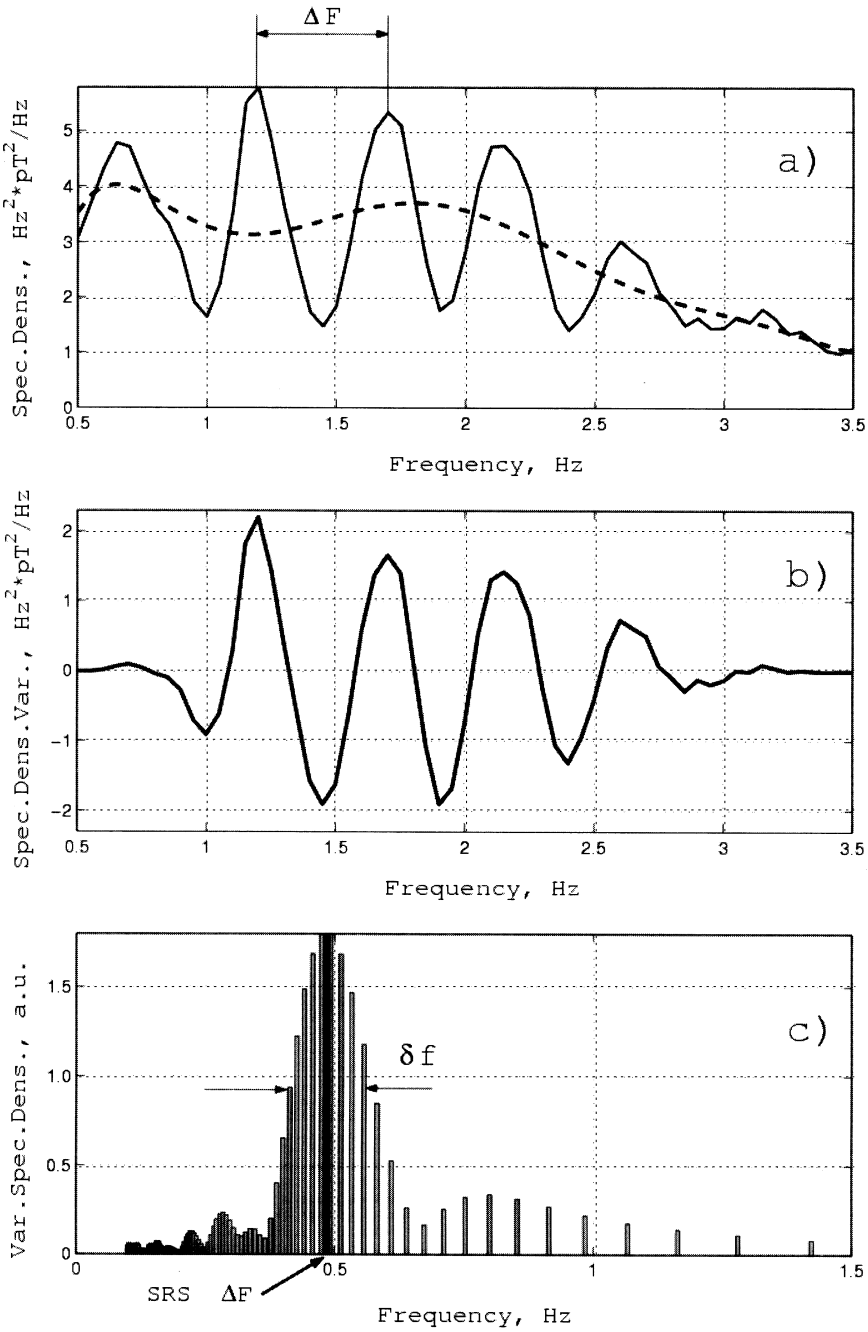

Fig. 3. The method of SRS identification and determination of the SRS parameters. (a) SRS (in solid line) and its trend (in dashed line), (b) SRS difference, and (c) Spectrum of the SRS difference. Its maximum location is the averaged ΔF in the SRS. SRS exists if the distribution is narrow banded, i.e. quality $Q > 1$.

- intensity of the resonance signal,
- "quality" parameter Q of the resonance structure.

The algorithm of data analysis is schematically shown in Fig. 3. The spectral resonance structure with the frequency difference ΔF is given in the top panel (a). Its 5-th order polynomial approximation is shown with a dashed line as a trend. The difference between the raw spectrum and its approximation (trend) (hereafter, we call it spectral density variation) is given in the middle panel (b).

The total power can be estimated as a sum of the resonant power and the background power approximately corresponding to the curve going through the minima of spectra in the top panel of Fig. 3. The intensity of the resonant signal is numerically estimated as the mean of the absolute value of spectral density variation. The relative inaccuracy of this approximation is low. Both spectra of the total signal and its resonant part have several approximately equidistant maxima. The average distance between the maxima is estimated with a help of Fourier transform of the spectrum of the resonant signal. This spectrum is shown in the bottom panel as a function of frequency. Its maximum corresponds to the averaged frequency difference between the SRS maxima. We define the "quality" Q of the resonant structure as the ratio of this maximal frequency to the halfwidth of the maximum δf using the formal similarity with the parameters of damping oscillations. A resonance structure by definition exists if at least two maxima are found in the spectrum, *i.e.* $Q > 1$. This allows us to exclude a possibility of false IAR detection caused by some other effects like Pc1 geomagnetic pulsations.

The IAR occurrence rate (occurrence probability) is defined as the ratio of number of nighttime (21–03 LT) intervals with our having observed SRS IAR to the total number of intervals, and this is plotted in the top panel. The average frequency difference between adjacent spectra maxima is shown in the bottom panel. The top of each grey rectangle means the average ΔF for a certain month, and the range of the dark rectangle indicates the error bar of estimation.

3. Seasonal and diurnal variations of the SRS parameters

The monthly averaged occurrence rate (or probability) of spectral resonance structure is shown in the upper panel of Fig. 4. The average frequency difference between the adjacent spectral maxima are summarized in the bottom panel of Fig. 4. When only one event was registered during a month, the frequency difference is not shown because of a big error in estimation. The seasonal variation averaged over all periods of observations of the IAR occurrence rate, frequency difference ΔF and intensity are shown in Fig. 5 from the top to the bottom. It is seen from the figures that during all the periods of observations the probability of IAR occurrence is maximal in autumn-winter and it vanishes in spring-early summer. A clear maximmum of ΔF is also observed in winter in the 2nd panal of Fig. 5. The bottom panel of Fig. 5 shows a broad maximum, so that we can say that the IAR power density depends relatively weakly on the season. So, the seasonal variations of the two quantities of IAR power and SRS IAR occurrence rate seem to be in anti-correlation with each other.

The diurnal variation of IAR occurrence rate for the four seasons is shown in Fig. 6 (winter, spring, summer and autumn, from top to the bottom). In winter and autumn when

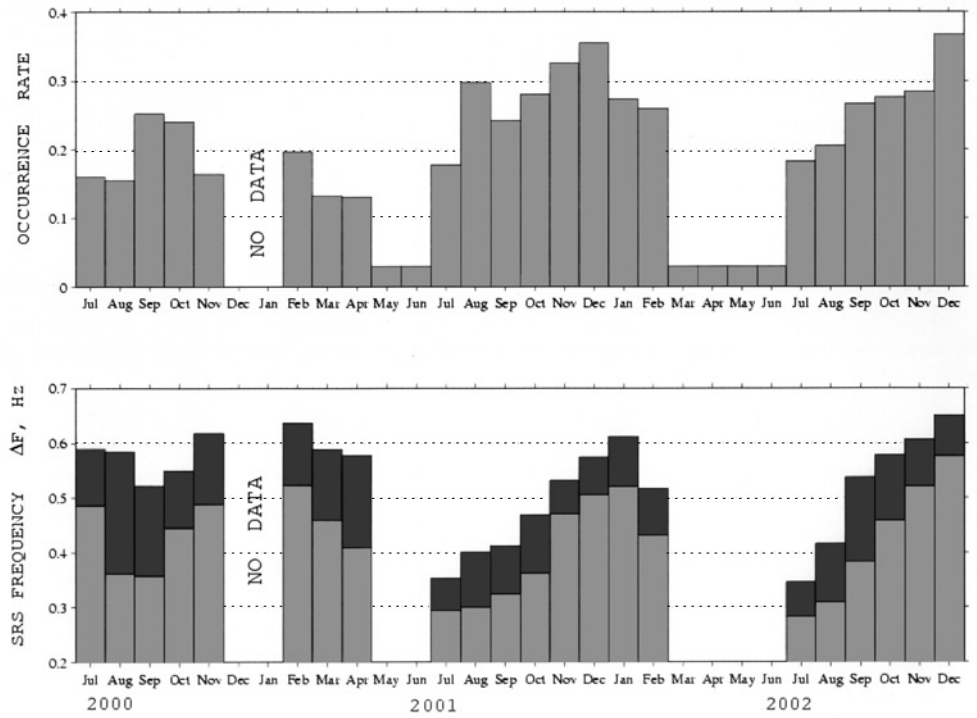

Fig. 4. The temporal evolution of monthly IAR occurrence rate (probability) during all the observation period from July 2000 to December 2002 (top panel). The bottom, the corresponding temporal variation of ΔF during the same period. The top of each grey rectangle indicates ΔF, and the range of dark rectangle means the error bar.

the occurrence rate is maximal there is a clear pre-midnight maximum. Besides, in winter a secondary weaker maximum is found at early morning (04–06 LT). Only few events were registered in spring, so that no estimates can be made for them. The IAR occurrence rate in summer seem to be shifted to the post-midnight hours.

4. SRS IAR and geomagnetic activity

SRS IAR occurrence rate at middle latitudes as well as at high latitudes (Yahnin *et al.*, 2003) is found to increase with the decrease in geomagnetic activity. This observational result is confirmed by our statistical analysis. Correlation coefficients of SRS occurrence rate with the *Kp* index of global magnetic activity for different 1-year intervals are shown in Fig. 7 (days with data gaps and the last three months, April–June 2002 (see seasonal dependence) were excluded from the analysis). The stable and reliable negative correlation of IAR with *Kp* is seen from the figure and it may be possible that SRS IAR are masked under disturbed geomagnetic conditions by the high background activity.

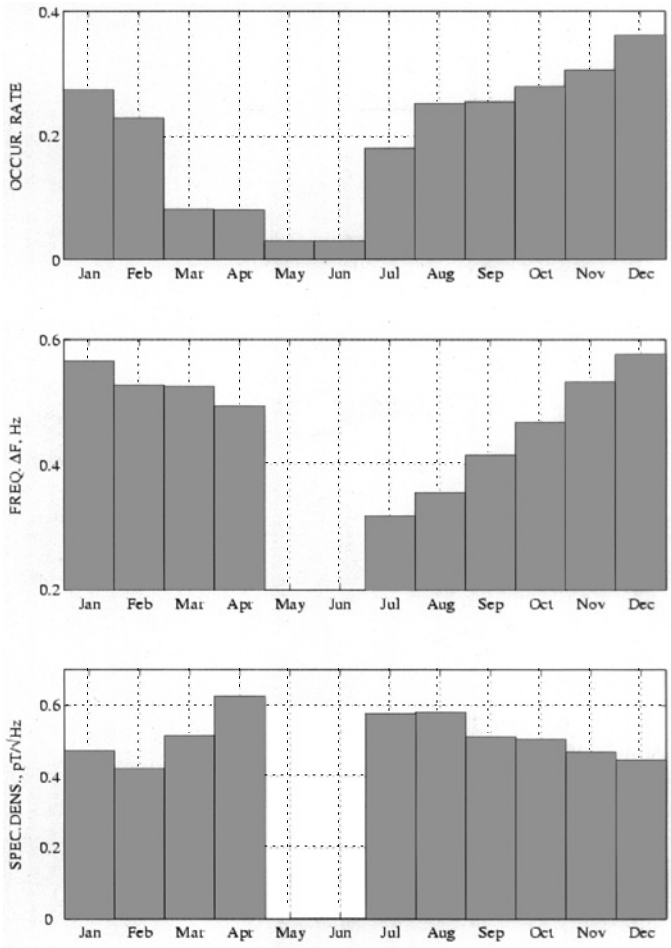

Fig. 5. Seasonal behavior of the occurrence rate (probability) (top), ΔF (middle) and power spectrum density (bottom) averaged over the observation period.

5. Discussion and conclusion

We characterize SRS by the fundamental frequency and averaged ΔF. The parameter Q characterizing the "quality" of the spectral resonance structure has been introduced. It is controlled by the IAR quality and the ratio of the amplitude of resonant signal to the background noise. If the resonance "quality" parameter exceeds some threshold value, we can detect any SRS IAR. We have found that the seasonal variation of the IAR occurrence rate is estimated based on the above detection criterion. The seasonal variation is strong: in spring–early summer only few SRS IAR events are registered, while the occurrence rate is found to strongly grow in autumn-winter (Fig. 6).

The main results of this paper can be summarized as follows.

1) Statistical properties of the IAR structures are analyzed for 2.5 years of observations.

IAR structures occur during approximately one quarter of the observation period (250 nights). There is an evident seasonal variation in the occurrence rate with the maximum in the autumn–winter period and almost a complete absence of IAR structures at the spring–early summer time.

2) The occurrence maximum in the diurnal variation is found at the LT of 21–23 h, and almost all the IAR structures are observed at local nighttime.
3) The averaged ΔF is about 0.2–0.5 Hz in the summer–autumn period, but it increases up to 0.5–0.7 Hz in the winter time;
4) SRS IAR are mostly polarized along the azimuthal direction (*D*-component). Diurnal variations in the two horizontal components are sometimes not identical.
5) IAR is found to be left-handed polarized.
6) There is anti-correlation of the IAR occurrence rate and *Kp* index of the global geomagnetic activity.

We compare the present experimental findings from the long-term observation at our middler latitude ($L=2.1$) station with the previous obervations at a high latitude ($L=5.2$)(Yahnin *et al*., 2003) and at a low latitude ($L=1.3$) (Bösinger *et al*., 2002). The observation by Yahnin *et al*. (2003) was based on an extremely long-term observation of about 5 years, while the observation by Bösinger *et al*. (2002) was performed only for half a year. When we think about the generation mechanism of IAR, the latitudinal dependence would be of essential importance. Several results have been reported on the basis of shorter data base (Belyaev *et al*., 1987, 1990) at middle latitude ($L=2.65$), but this paper provides the first results of middle latitude IAR characteristics by using the sufficiently long-term observation. In contrast to the previous results at high and middle latitudes, Point (1) in our summary suggests that IAR strucures occur approxinately one quarter of the observation periods (250 nights). This

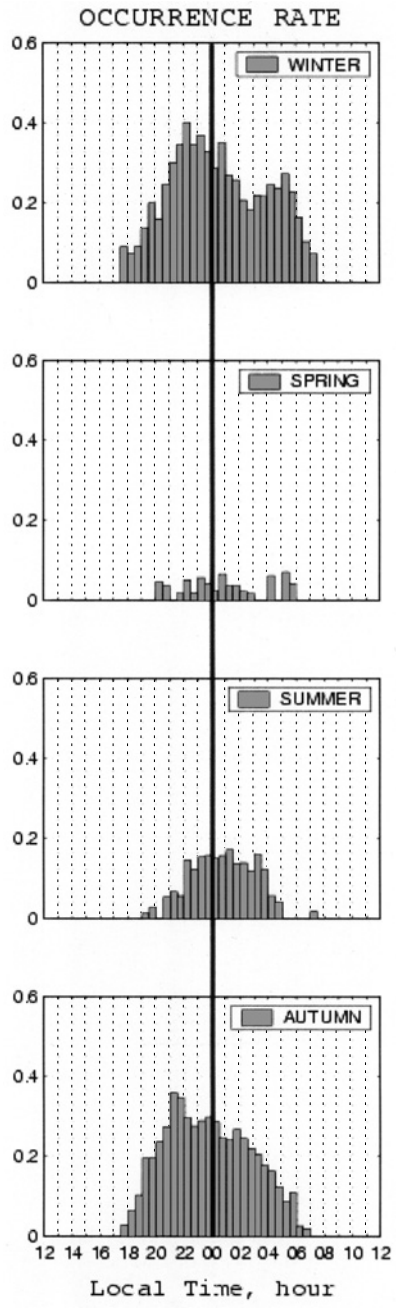

Fig. 6. Diurnal variation (or local time dependence) of the IAR occurrence rate for the different seasons (winter, spring, summer and autumn, from top to the bottom).

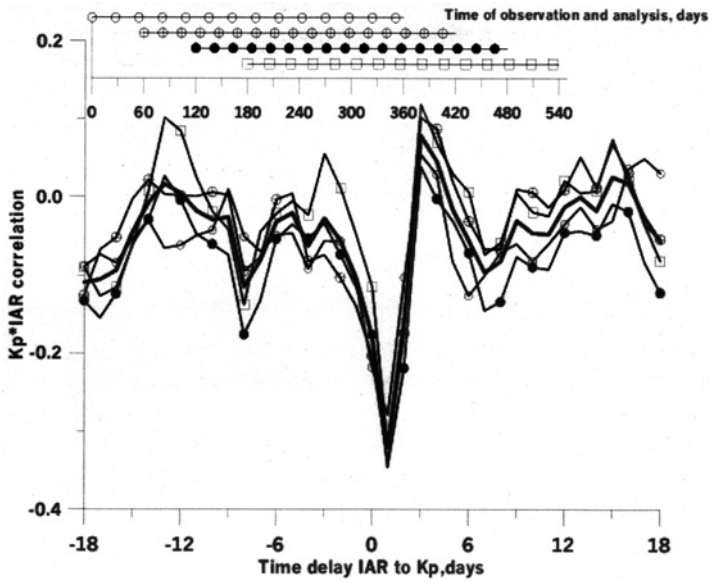

Fig. 7. Correlation coefficients of the IAR occurrence rate with the Kp index for different one-year periods (shown above). All the correlation coefficients are negative for time delay of 0–1 day.

means that the IAR phenomena are not so rare, but that they are rather regular phenomena. This point seems to be close to and be consistent with the conclusion by Bösinger *et al*. (2002) at low latitude.

According to the common view, the main source of the IAR excitation is the activity of the global thunderstorm centers. However, this activity seems to depend on the season only weakly (Nickolaenko and Hayakawa, 2002) and the observed strong seasonal variation of IAR occurrence rate seems to be unexplainable by this assumption. We here assume the possible existence of an additional source of excitation of the IAR resonance structures: the fluctuations of neutral gas velocity at the heights of the ionospheric *E*-layer. Neutral wind height-dependent seasonal variation with winter amplitude maximum and minimum in spring-early summer (Manson *et al*., 1999). The velocities are found to vary from several tens to about one hundred m/s in dependence on the local time, season and height. The seasonal variation of the neutral wind velocity is qualitatively similar to the observed seasonal variation of the IAR occurrence rate. Further details on this mechanism with numerical estimations will be published elsewhere.

Acknowledgments

This research was partially supported by ISTC under Grant 1121 and by Commission of the EU (grant No. INTAS-01-0456). Two authors (O.A.M. and M.H.) are thankful for the support from International Space Science Institute (ISSI) at Bern, Switzerland within the project “Earthquake influence on the ionosphere as evident from satellite density-electric field data”. One of the authors (M.H.) is grateful to the Mitsubishi Foundation for its sup-

port.

The editor thanks Dr. A. P. Nickolaenko and another referee for their help in evaluating this paper.

References

Alpert, Ya. L. (1974): Propagation of Radio Waves in the Ionosphere. New York, Plenum Press.

Belyaev, P.P., Polyakov, S.V., Rapoport, V.O. and Trakhtengertz, V.Y. (1987): Discovery of the resonance spectrum structure of atmospheric electromagnetic noise background in the range of short-period geomagnetic pulsations. Dokl. Akad. Nauk SSSR, **297**, 840–846.

Belyaev, P.P., Polyakov, S.V., Rapoport, V.O. and Trakhtengertz, V.Y. (1990): The ionospheric Alfvén resonator. J. Atmos. Terr. Phys., **52**, 781–788.

Belyaev, P.P., Bösinger, T., Isaev, S.V. and Kangas, J. (1999): First evidence at high latitudes for the ionospheric Alfvén resonator. J. Geophys. Res., **104**, 4305–4317.

Bösinger, T., Haldoupis, C., Belyaev, P.P., Yakunin, N.V., Semenova, Demekhov, A.G., and Angelopoulos, V. (2002): Spectral properties of the ionospheric Alfvén resonator observed at a low-latitude station (L=1.3). J. Geophys. Res., **107**, A10, 1281, doi:10.1029/2001JA005076.

Demekhov, A.G., Trakhtengertz, V.Yu. and Bösinger, T. (2000a): Pc 1 waves and ionospheric Alfvén resonator: Generation or filtration? Geophys. Res. Lett., **27**, 3805–3808.

Demekhov, A.G., Belyaev, P.P., Manninen, J., Turunen, T. and Kangas, J. (2000b): Modeling the diurnal evolution of the resonance spectral structure 12 of the atmospheric noise bacground in the PC 1 frequency range. J. Atmos. Solar-Terr. Phys., **62**, 257–265.

Gladychev, V., Baransky, L., Schekotov, A., Fedorov, E., Pokhotelov, O., Andreevsky, S., Rozhnoi, A., Khabazin, Y., Belyaev, G., Gorbatikov, A., Gordeev, E., Chebrov, V., Sinitsin, V., Lutikov, A., Yunga, S., Kosarev, G., Surkov, V., Molchanov, O., Hayakawa, M., Uyeda, S., Nagao, T., Hattori, K. and Noda, Y. (2002): Some preliminary results of seismo-electromagnetic research at Complex Geophysical Observatory, Kamchatka. Seismo Electromagnetics: Lithosphere—Atmosphere—Ionosphere Coupling, ed. by M. Hayakawa and O.A. Molchanov. Tokyo, Terra Sci. Publ., 421–432.

Lysak, R.L. (1991): Feedback instability of the ionospheric resonator cavity. J. Geophys. Res., **96**, 1553–1568.

Manson, A., Meek, C., Hagan, M., Hall, C., Hocking,W., MacDougall, J., Franke, S., Riggin, D., Fritts, D., Vincent, R. and Burrage, M. (1999): Seasonal variations of the semi-diurnal and diurnal tides in the MLT: multi-year MF radar observations from 2 to 70°N, and the GSWM tidal model. J. Atmos. Solar-Terr. Phys., **61**, 809–828.

Nickolaenko, A.P. and Hayakawa, M. (2002): Resonances in the Earth-Ionosphere Cavity. Dordrecht, Kluwer, 380 p.

Polyakov, S.V. (1976): On the properties of the ionospheric Alfvén resonator. KAPG Symposium on Solar-Terrestrial Physics, Vol. 3. Moscow, Nauka, 72–73.

Polyakov, S.V. and Rapoport, V.O. (1981): The ionospheric Alfvén resonator. Geomagn. Aeron., **21**, 610–614.

Pokhotelov, O.A., Pokhotelov, D., Strelkov, A., Khruschev, V. and Parrot, M. (2000): Dispersive ionospheric Alfvén resonator. J. Geophys. Res., **105**, 7737–7746.

Pokhotelov, O.A., Khruschev, V., Parrot, M., Senchenkov, S. and Pavlenko, V.P. (2001): Ionospheric Alfvén resonator revisited: Feedback instability. J. Geophys. Res., **106**, 25813–25823.

Trakhtengertz, V.Y. and Feldstein, A.Y. (1991): Turbulent Alfvén boundary layer in the polar ionosphere, 1. Excitation conditions and energetics. J. Geophys. Res., **96**, 19363–19374.

Trakhtengertz, V., Demekhov, A.G., Polyakov, S.V. and Rapoport, V.O. (2000a): A mechanism of PC 1 pearl formation based on the Alfvén sweep maser. J. Atmos. Solar-Terr. Phys., **62**, 231–238.

Trakhtengertz, V.Yu., Belyaev, P.P., Polyakov, S.V., Demekhov, A.G., and Bösinger, T. (2000b): Excitation of Alfvén waves and vorticies in the ionospheric Alfvén resonator by modulated powerful radio waves. J. Atmos. Solar-Terr. Phys., **62**, 267–276.

Uyeda, S., Nagao, T., Hattori, K., Noda, Y., Hayakawa, M., Miyaki, K., Molchanov, O., Gladychev, V., Baransky, L., Schekotov, A., Belyaev, G., Fedorov, E., Pokhotelov, O., Andreevsky, S., Rozhnoi, A., Khabazin, Y., Gorbatikov, A., Gordeev, E., Chebrov, V., Lutikov, A., Yunga, S., Kosarev, G. and Surkov, V. (2002):

Russian-Japanese complex geophysical observatory in Kamchatka for monitoring of phenomena connected with seismic activity. Seismo Electromagnetic: Lithosphere—Atmosphere—Ionosphere Coupling, ed. by M. Hayakawa and O.A. Molchanov. Tokyo, Terra Sci. Publ., 413–419.

Yahnin, A.G., Semenova, N.V., Ostapenko, A.A., Kangas, J., Manninen, J. and Turunen, T. (2003): Morphology of the spectral resonance structure of the electromagnetic background noise in the range of 0.1–4 Hz at L = 5.2. Ann. Geophys., **21**, 779–786.